

## Chapter 2

# Microdialysis for Vitreal Pharmacokinetics

Ravi D. Vaishya, Hari Krishna Ananthula, and Ashim K. Mitra

**Abstract** Microdialysis has been an instrumental sampling technique to study ocular pharmacokinetics without sacrificing a huge number of animals. It has undergone significant transformations in the last decade and several animal models have been established for sampling inaccessible posterior segment tissues such as vitreous humor. Remarkable progress has been made in the probe design and validation techniques. In the following chapter we have discussed the principle and development of various animal models related to posterior segments.

### Abbreviations

ACV	Acyclovir
AZdU	3'-Azido-2',3'-dideoxyuridine
AZT	Zidovudine
E17βG	17-β-glucuronide
GCV	Ganciclovir
PLGA	Poly(DL-lactide-co-glycolide)
PLGA-PEG-PLGA	Poly(DL-lactide-co-glycolide)-poly(ethylene glycol)-poly(DL-lactide-co-glycolide)
VACV	Val-acyclovir
VVACV	Val-val-acyclovir

---

A.K. Mitra(✉)

Division of Pharmaceutical Sciences, University of Missouri-Kansas City, School of Pharmacy,  
2464 Charlotte Street (HSB-5258), Kansas City, MO 64108-2718, USA  
e-mail: mitraa@umkc.edu

## 2.1 Introduction

Several retinal diseases such as diabetic macular edema, retinoblastoma and age-related macular degeneration require chronic treatments. Usually therapeutics is delivered by intravenous, subconjunctival, intravitreal (IVT) or peribulbar routes. Precise knowledge of various pharmacokinetic parameters is necessary for designing a dosage regimen. Drug release from sustained release formulations must be modulated so that drug level can be precisely maintained within the therapeutic window at the target site. The target site is usually retina, Bruch's membrane and choroid for most posterior segment diseases. However, it is impossible to measure drug concentrations at these sites unless the animal is sacrificed and tissues are assayed for drug concentrations. However, in order to construct a pharmacokinetic profile by this method, 6–20 animals for each time interval with at least ten time points are necessary to adequately define the absorption, distribution and elimination processes. Overall, 120–150 animals are required for single dose pharmacokinetic study. In this scenario, microdialysis offers an important sampling technique that can be an alternative method to avoid the use of huge number of animals. It can also allow continuous sampling. Previously, microdialysis has been extensively applied to measure concentrations of drugs or endogenous substances such as neurotransmitters in the brain and eye. So far this method has been employed for sampling body fluids including blood, vitreous humor, aqueous humor and extracellular fluids. Since late 1980s, the technique has undergone several major modifications for sampling analytes in vitreous as well as aqueous humor.

Microdialysis was utilized by Kalant et al. (1958) to measure steroid concentration in the blood. In mid 1970s, neuroscientists modified the technique for measuring concentration of dopamine in rat brain (Ungerstedt and Pycocock 1974). In 1987, Gunnarson et al. for the first time employed microdialysis to measure free amino acids in the vitreous humor of albino rabbits (Gunnarson et al. 1987). Since then, various investigators have employed microdialysis to understand pharmacokinetics of drugs as well as endogenous substances in vitreous fluid. So far, rabbits, rats, cats and pigeons have been utilized for vitreal microdialysis, although rabbits represent the most widely employed animal model. In the following sections, the advancements in the technique and its applications in posterior segment pharmacokinetics have been discussed.

## 2.2 Posterior Segment as a Sampling Site

Vitreous chamber is the sampling site for posterior segment microdialysis. It represents a connective tissue consisting of ~99% water with dissolved chondroitin sulfate, collagen, mucopolysaccharides such as glycosaminoglycans and hyaluronates providing gelatinous consistency (Rittenhouse and Pollack 2000). In adults no vitreous humor is regenerated (Rittenhouse and Pollack 2000). In the posterior segment, the photoreactive tissue i.e., retina is nourished by choroidal and retinal

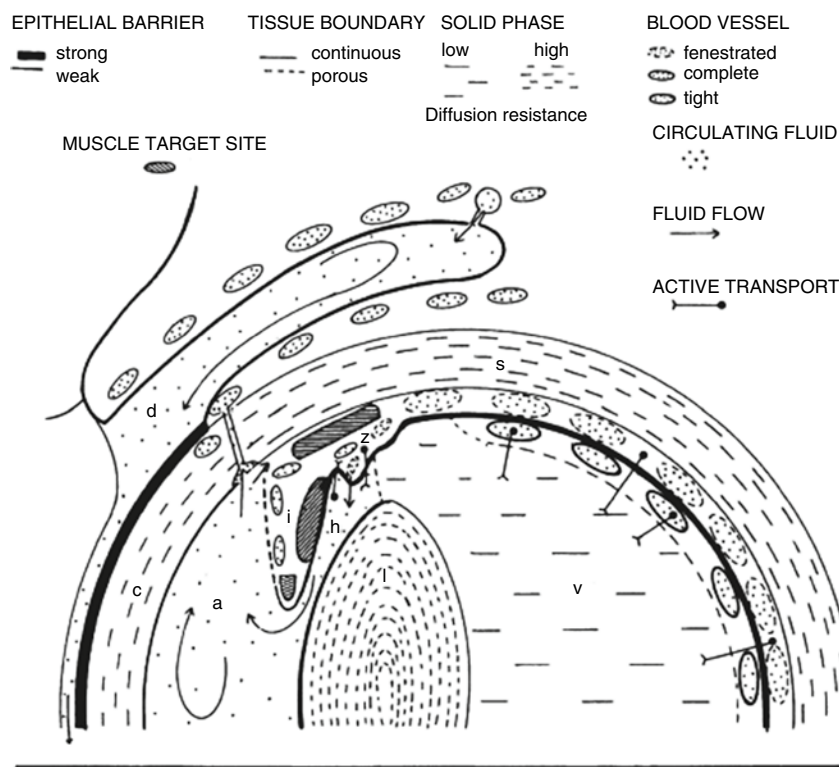


**Fig. 2.1** Diagrammatic representation of the routes of elimination of drugs from the vitreous of the eye

blood vessels. Movement of nutrient and waste molecules from the blood to retina is controlled by specific transport systems (Fig. 2.1). However, movement of these molecules such as amino acids and neurotransmitters to and within vitreous humor is via simple diffusion (Fig. 2.1) (Gunnarson et al. 1987). With respect to mass transfer, vitreous humor can be viewed as unstirred static fluid (Hughes et al. 1996). The globe is a closed system and does not allow sampling of tissues without irreversible damage. In such case, microdialysis plays an important role as a sampling technique which significantly reduces the number of animals required for pharmacokinetic studies.

## 2.3 Principle of Microdialysis

Microdialysis works on the principle of dialysis wherein a microdialysis probe is inserted in the tissue or fluid of interest. The probe has a semipermeable dialysis membrane which is circulated with physiological solution at a constant flow rate (Fig. 2.2).

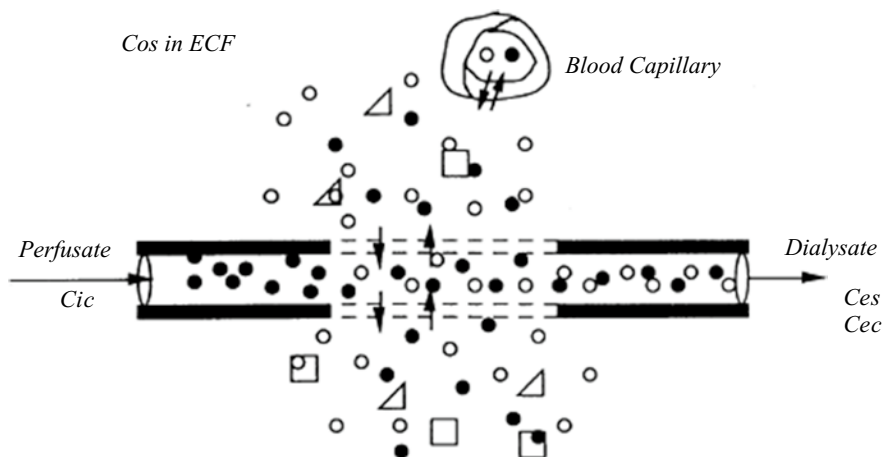


**Fig. 2.2** Microdialysis schematics. Microenvironment within and surrounding the microdialysis probe in vivo. The *solid* and *dashed* line segments schematically represent the non-permeable probe wall and semipermeable membrane, respectively. *Open* and *filled circles* represent molecules of solute of interest and retrodialysis calibrator, respectively. *Squares* and *triangles* represent macromolecules which may bind solute and or calibrator but which are not recovered by dialysis. *Arrows* indicate the direction of transport

Following insertion of microdialysis probe, the concentration gradient across the semipermeable membrane causes the solute to diffuse in or out of dialysis probe. In order to avoid change in composition (ionic strength) of the surrounding fluid, the composition of perfusate should be similar to the fluid surrounding the dialysis membrane. Movement of solute molecules is also dependent on the molecular weight cut off (MWCO) of dialysis membrane. The process, governed by concentration gradient, never reaches the equilibrium since the perfusate is constantly circulated through the probe. Therefore, concentration in the dialysate is not same as that of vitreous. Analyte concentration in the dialyzing fluid (vitreous humor) can be determined from recovery, also known as extraction efficiency or relative recovery.

### 2.3.1 Extraction Efficiency/Recovery

Recovery is a ratio between the concentration of analyte in dialysate ( $C_{out}$ ) and fluid surrounding the probe ( $C_{in}$ ). The concentration of analyte in dialysate is a fraction of that present in the fluid surrounding the probe. Therefore, in vitro probe recovery is a key parameter for analyzing in vivo microdialysis data. In vitro probe recovery may be calculated by (2.1).

$$\text{Recovery}_{\text{in vitro}} = \frac{C_{out}}{C_{in}}. \quad (2.1)$$

Following determination of recovery with defined parameters such as flow rate, (2.2) can be utilized to transform dialysate concentration ( $\hat{C}_{out}$ ) into actual vitreous concentration ( $\hat{C}_{in}$ ).

$$\hat{C}_{in} = \frac{\hat{C}_{out}}{\text{Recovery}_{in vitro}}. \quad (2.2)$$

*Absolute recovery* is the amount of analyte over a definite period of time. It is the product of relative recovery ( $R$ ), flow rate ( $F$ ) and concentration of the analyte ( $C$ ) (Wages et al. 1986).

Relative recovery can also be calculated by retrodialysis. In this method, an internal standard is perfused through dialysis tube and the loss in internal standard is measured along with the analyte from the dialysate. Recovery of both analyte and internal standard are calculated. Recovery, fractional loss of internal standard during dialysis, is calculated with (2.3).

$$\text{Recovery}_{internal standard} = \frac{C_{in} - C_{out}}{C_{in}}, \quad (2.3)$$

$C_{in}$  is the concentration of internal standard entering probe;  $C_{out}$  is the concentration of internal standard exiting the probe. Recovery of the internal standard and analyte can be compared taking ratio, given in (2.4).

$$\text{Recovery ratio} = \frac{\text{Recovery}_{internal standard}}{\text{Recovery}_{analyte}}, \quad (2.4)$$

A number of factors may influence in vitro probe recovery including perfusate flow rate and composition, temperature, properties of the membrane, probe design, analyte concentration and molecular weight. For example, the relative recovery decreases as the perfusate flow rate is raised (Wages et al. 1986). Among these, temperature and flow rate of perfusate are most critical factors influencing in vitro recovery. Wang et al. studied the relationship between perfusate flow rate and in vitro recovery utilizing zidovudine (AZT) as analyte and 3'-azido-2',3'-dideoxyuridine (AZdU) as internal standard. Recovery decreased exponentially with the increase in flow rate (Wang et al. 1993) (Fig. 2.3). Therefore, the rate of perfusate in dialysis probe is a key parameter that needs to be considered while optimizing microdialysis parameters. Usually a flow rate of 2  $\mu\text{L}/\text{min}$  is preferred for most experiments. Figure 2.4 explains the influence of temperature on recovery at different perfusate flow rates (Wages et al. 1986). Recovery of DOPAC was studied by retrodialysis and effect of temperature on recovery was examined. Recovery was highest at 37°C and least at 23°C. This difference may be attributed to elevation in diffusion coefficient with rising temperature (Wages et al. 1986).

It has been well documented that in vivo recovery is always less than in vitro recovery during brain microdialysis studies (Amberg and Lindefors 1989). This may lead to misinterpretation of drug concentration data. During brain microdialysis, the

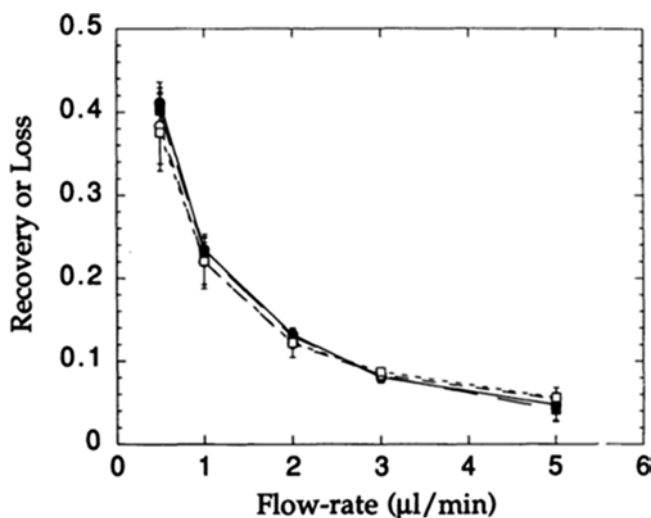


**Fig. 2.3** Effect of flow rate on in vitro recovery of zidovudine (AZT) and loss of 3'-azido-2',3'-dideoxyuridine (AZdU) during microdialysis and retrodialysis. *Filled square and circle* represents loss of AZT and AZdU. *Empty square and circle* represents recovery of AZT and AZdU

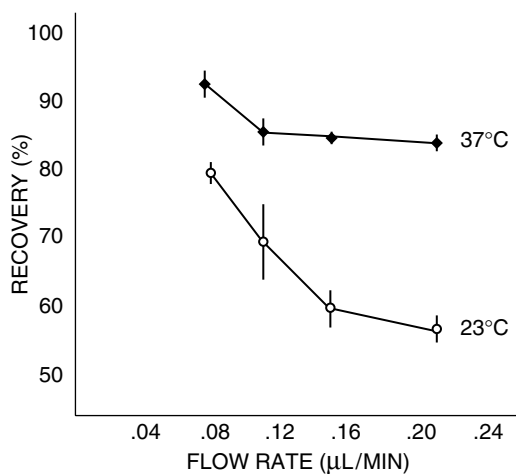


**Fig. 2.4** Effect of temperature on in vitro recovery of DOPAC at different flow rates by retrodialysis

analyte concentration is measured in the extracellular fluid. Substrate diffuses from interstitial space in a tortuous path. Moreover, the analyte may partition inside the cells and therefore its concentration in the dialysate may not reflect the actual concentration when tissues are sampled with microdialysis. Movement through tortuous path and partitioning into cells may lower in vivo recovery of substrate.

However, this is not the case with vitreous humor since it is uniform and has insignificant radial or spherical dependence on diffusion coefficient of substrates (Maurice 1957). This is because vitreous humor is >99% water and solid content (collagen fibrils) is about 0.2%. At such a low concentration, distance between two collagen fibrils is 2  $\mu\text{m}$ , which would not hinder the diffusion of molecules in vitreous (Maurice 1959). Therefore, the rate of diffusion of a molecule in vitreous humor remains the same as in free solution despite the viscous nature of vitreous fluid.

## 2.4 Posterior Segment Microdialysis: Development of Models and Applications

Invasive nature of microdialysis procedure has restricted its application to animals. Various species have been employed to develop and validate microdialysis model, including rats (Katayama et al. 2006; Hosoya et al. 2009), rabbits, cats (Ben-Nun et al. 1988), zebrafish (Puppala et al. 2004) and pigeon (Adachi et al. 1995, 1998). Rabbits have been the animal model of choice for vitreal pharmacokinetics and it had been widely used for in vivo studies involving amino acid and neurotransmitter release (Gunnarson et al. 1987). More importantly, rabbits have fairly large posterior segment with adequate vitreous humor volume (1–1.5 mL) to allow probe implantation. However, it differs from human eyes in several aspects such as absence of macula, lower corneal thickness, slower blinking reflex, avascular retina and the absence of uveoscleral outflow pathway (Rittenhouse and Pollack 2000). All these differences must be taken into account while reporting the pharmacokinetic data. Rabbit models developed so far can be divided into two main categories (a) anesthetized animal model, (b) conscious animal model.

### 2.4.1 Anesthetized Animal Models

Microdialysis has been a well-established technique to study neurotransmitter release in brain. In late 1980s, several investigators employed microdialysis to understand neuro-biochemistry and visual function by measuring released endogenous factors. Also the effects of various experimental conditions such as ischemia and laser photocoagulation were investigated by pharmacokinetics of specific markers.

Gunnarson et al. (1987) sampled preretinal vitreous humor to identify and quantify amino acids. The design of probes was derived from the probes used in brain microdialysis, where dialysis probe was mounted on stainless-steel cannula. Louzada-Junior et al. (1992) studied the effects of ischemia on the release of excitatory amino acids (EAAs), like glutamate, into vitreous. These investigators observed a strong correlation between release of glutamate during reperfusion and cell death. In another study, Stempels et al. (1994) performed vitreal microdialysis to determine the concentration of released catecholamines, following laser photocoagulation of the retina at a particular wavelength.

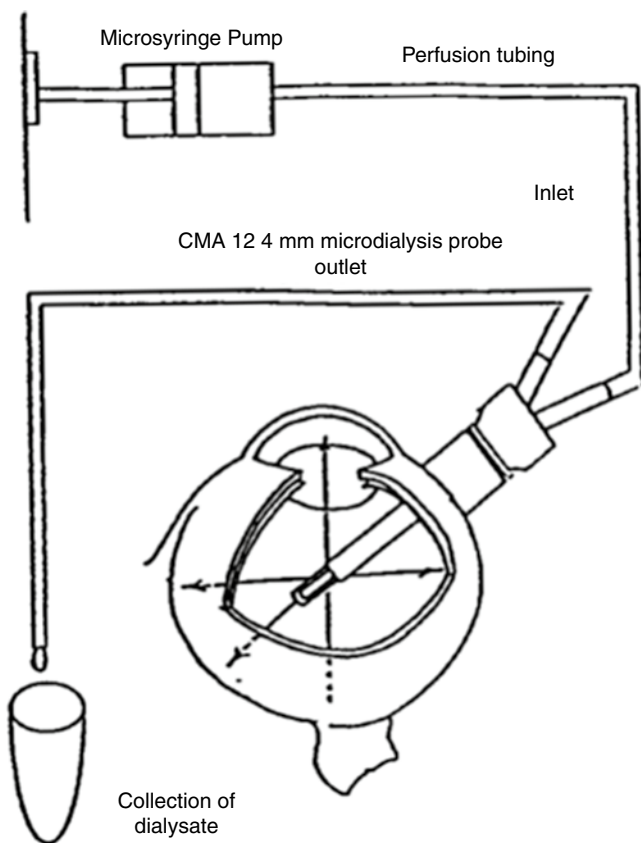


**Fig. 2.5** Schematic representation of position of the probe in vitreal chamber

Microdialysis was also employed for developing pharmacokinetic profile of acyclovir (ACV) and ganciclovir (GCV) following IVT administration in anesthetized rabbit model (Hughes et al. 1996). New Zealand albino and Dutch-belted pigmented rabbits were employed in the study. Briefly, rabbits were anesthetized and a siliconized probe guide (guide cannula) was inserted 3–4 mm below the limbus into vitreous chamber. Guide cannula was positioned in vitreous and fixed on sclera with cyanoacrylate adhesive. A 100  $\mu\text{L}$  of ACV or GCV solution was administered by IVT bolus injection followed by insertion of microdialysis probe through probe guide. Isotonic phosphate buffer saline (IPBS) solution (pH 7.4) was perfused at a flow rate of 2  $\mu\text{L}/\text{min}$  with a microdialysis syringe pump (CMA 112). A schematic representation of probe position in vitreal chamber is shown in Fig. 2.5.

Various pharmacokinetic parameters have been summarized in Table 2.1. Vitreal concentration time profiles may be explained by initial diffusion and distribution, followed by continuous elimination from vitreous along with possible distribution into surrounding compartments. Vitreal elimination half-lives for ACV and GCV were



**Table 2.1** Comparison of intravitreal (IVT) pharmacokinetic parameters in albino and pigmented rabbits following IVT administration of the nucleoside analogs

Compound [dose ( $\mu\text{g}$ )]	Albino rabbits		Pigmented rabbits	
	Acyclovir (ACV) [200]	Ganciclovir (GCV) [200]	ACV [200]	GCV [200]
$K_{el} \times 10^3 \text{ (min}^{-1}\text{)}$	3.89 (0.41)	4.54 (0.83)	1.41 (0.25)	2.10 (0.36)
$t_{1/2} \text{ (h)}$	2.98 (0.24)	2.62 (0.44)	8.36 (1.39)	5.59 (0.92)
$V_d \text{ (mL)}$	0.99 (0.21)	1.05 (0.29)	6.73 (1.71)	3.71 (1.64)
AUC (mM min/mL)	150.5 (20.5)	109.8 (25.7)	100.1 (29.3)	105.0 (38.0)
MRT (min)	248.9 (23.2)	170.7 (31.1)	842.1 (69.6)	539.6 (58.4)

$2.98 \pm 0.24$  and  $2.62 \pm 0.44$  h, respectively. Lipophilic molecules and molecules with active transport mechanism have been reported to clear from vitreous via distribution in the peripheral compartment through retina/choroidal circulation (Hughes et al. 1996). Because of large surface area of retina, clearance is faster and hence half-life is 2–5 h. The hydrophilic molecules and large molecular weight compounds diffuse through retrozonular space and are eliminated via aqueous humor and hence usually show longer half-lives ranging from 20 to 30 h. Short half-lives of ACV and GCV in vitreous strongly supported the transretinal mechanism for their clearance. For both drugs, the mean residence time (MRT), half-life and volume of distribution ( $V_d$ ) were significantly higher in pigmented rabbits compared to albino rabbits (Table 2.1). The vitreous humor volume in rabbits is 1–1.5 mL and  $V_d$  for ACV and GCV is 6.73 and 3.71 mL, respectively. Higher  $V_d$  in pigmented rabbits can be explained by drug binding with melanin pigments, which are absent in albino rabbits. With the help of microdialysis technique vitreal elimination half-lives for ACV and GCV were determined with remarkable reproducibility and the influence of protein binding was delineated.

Knowledge of elimination pharmacokinetics from vitreous humor is vital for designing dosage regime for posterior segment diseases. Vitreal elimination mechanism of molecules depends largely on the physicochemical parameters like hydrophilicity, lipophilicity ( $\log P$ ), size of the molecule and diffusivity of the molecule in vitreous fluid. Molecules may be substrates for transporters expressed on retinal pigmented epithelium (RPE) or retinal blood capillaries, which may also determine vitreal half-life. The disposition mechanism may be transretinal or via aqueous humor after IVT injection, as discussed earlier. Therefore, in order to explain drug elimination from vitreous chamber, aqueous humor concentration should also be measured. Macha and Mitra 2001 developed a novel dual probe microdialysis method in anesthetized animals, which allowed sampling of both aqueous humor and vitreous humor simultaneously. The aqueous humor was implanted with linear probe with a 25-G needle. A concentric probe was implanted in vitreous chamber with 22-G needle. A schematic representation of probes positioning in both chambers is shown in Fig. 2.6. Probe implantation in aqueous humor decreased IOP due to small amount of aqueous humor loss. Therefore, animals were allowed a recovery period of 2 h so that IOP reverts to normal. IOP returned to baseline level within 1 h

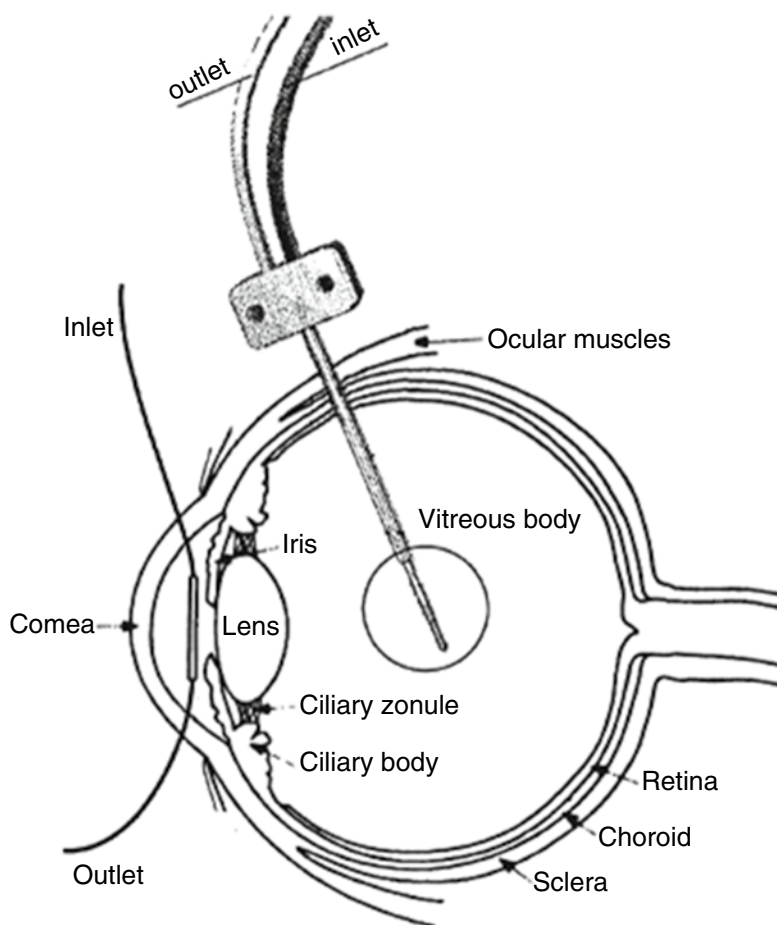


**Fig. 2.6** Diagrammatic representation of the microdialysis probes implanted in the anterior chamber and vitreous of the eye

following probe implantation in aqueous humor. In order to ensure the integrity of the blood ocular barriers (BOB), protein concentration was measured in aqueous and vitreous humor after probe insertion. There was no significant rise in protein levels in both aqueous and vitreous humor. Elimination kinetics of fluorescein was studied in aqueous and vitreous humor following IVT and systemic administration to examine the integrity of BOB. The concentration time profiles of fluorescein following systemic and IVT injection are shown in Figs. 2.7 and 2.8, respectively.

Fluorescein achieved higher aqueous humor levels compared to vitreous after systemic administration. Fluorescein entered aqueous humor via iris/ciliary blood supply due to rapid capillary diffusion. The permeability index of anterior chamber was 9.48% and that of vitreal chamber was 1.99%. High permeability index of anterior chamber explains relatively free movement of fluorescein between plasma and aqueous humor. Thus, dual probe microdialysis model was validated by protein

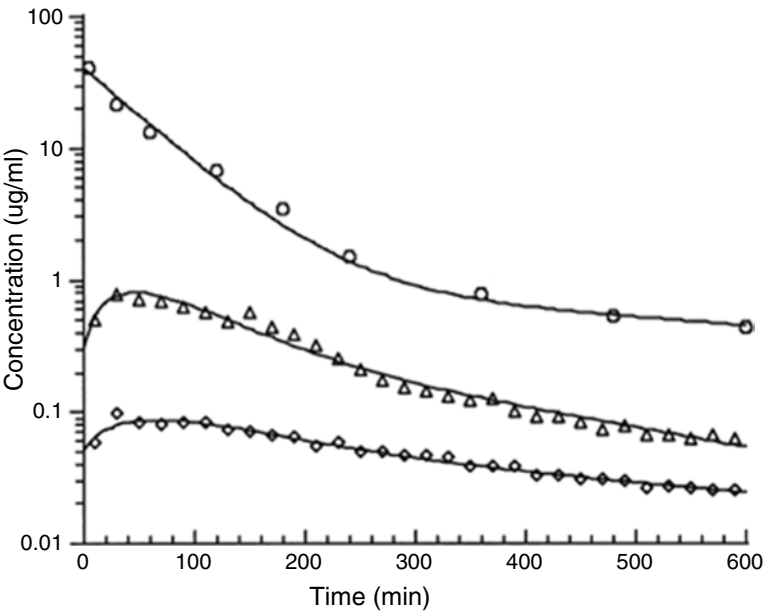


**Fig. 2.7** Concentration-time profiles of plasma, anterior chamber and vitreous fluorescein after systemic administration (10 mg/kg). *Open circle* represent plasma concentrations, *open triangle* aqueous and *open diamond* vitreous concentrations. The *line* drawn represents the non-linear least-squares regression fit of the model to the concentration-time data

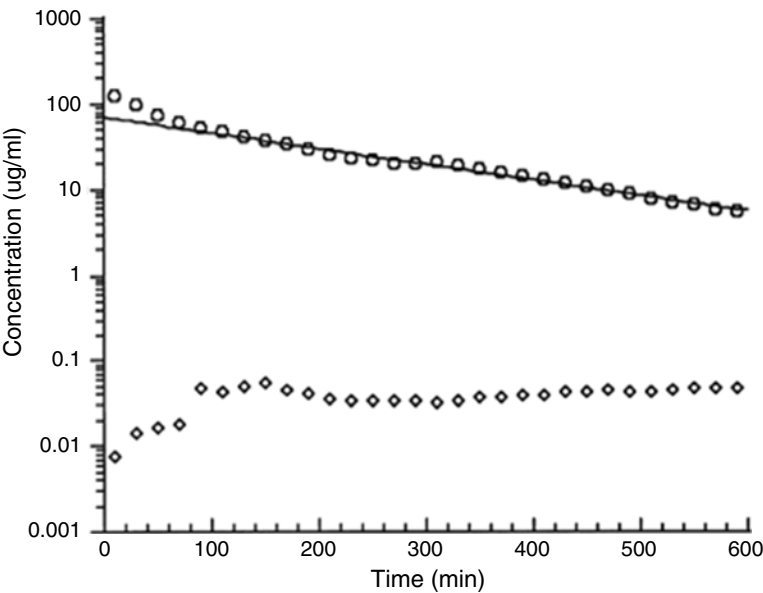


**Fig. 2.8** Concentration-time profile of vitreous and anterior chamber fluorescein after intravitreal administration (100 µg). *Open circle* represent vitreous and *open diamond* aqueous concentrations. The *line* represents the non-linear least-squares regression fit of the model to the concentration-time data

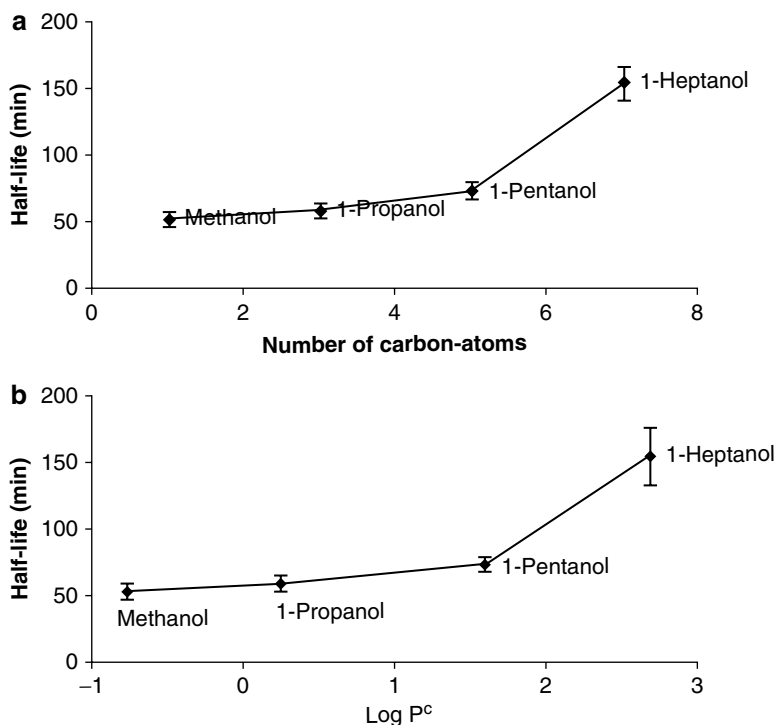


**Fig. 2.9** (a) Vitreal elimination half-life vs. number of carbon atoms in the alcohol molecule. (b) Intravitreal half-life vs. log P of alcohols. Error bars represent SD for  $n=4$

concentration measurements and fluorescein pharmacokinetics in both chambers and IOP measurements in aqueous humor. The model permitted simultaneous monitoring of both aqueous and vitreous humor drug concentrations. Later on, the method was employed by several investigators to enlighten the importance of physicochemical properties and the involvement of transporters in vitreal elimination.

Atluri and Mitra (2003) studied the effect of lipophilicity on vitreal pharmacokinetics using short-chain aliphatic alcohols by performing dual probe microdialysis. Various length of short-chain alcohols including methanol, 1-propanol, 1-pentanol and 1-heptanol were injected intravitreally. Vitreal and aqueous humor pharmacokinetic parameters were measured to delineate mechanism of elimination from vitreous chamber. Ideally, half-life should decrease with the increment in lipophilicity because of increase in permeability across retina. Surprisingly, vitreal elimination half-lives were found to be longer with increment in chain length and log P (Fig. 2.9). Also, the increment in half-life from 1-pentanol to 1-heptanol was remarkable compared to methanol to 1-pentanol. This increment in half-life may be attributed to decrease in diffusivity of molecules in hydrophilic vitreous as well as decrease in permeability across retina because of high lipophilicity of 1-heptanol (log P ~7). Time required to reach maximum concentration in aqueous humor also increased

with an increase in lipophilicity of molecules, possibly due to decrease in diffusivity. 1-Heptanol could not achieve detectable level in aqueous humor because of its high lipophilicity. Thus, decreased vitreal diffusivity and transretinal permeability may significantly influence vitreal disposition of highly lipophilic molecules.

Macha et al. (2001) studied vitreal disposition kinetics of diester prodrugs of GCV upon IVT administration using dual probe microdialysis. The disposition of prodrugs was dependent on the enzymatic degradation (esterase and peptidase enzymes) and diffusion mediated elimination. Diester prodrug enzymatically degraded into their respective monoester, which subsequently hydrolyzed to active parent drug GCV. The concentrations of GCV diester, GCV monoester and parent molecule GCV after IVT injection were measured by microdialysis and pharmacokinetic parameters were calculated. Because of enzymatic degradation, the vitreal elimination half-lives of GCV prodrugs decreased from GCV diacetate ( $112 \pm 37$  min)  $\rightarrow$  GCV dipropionate ( $41.9 \pm 13.1$  min)  $\rightarrow$  GCV dibutyrate ( $33.5 \pm 6.5$  min), despite an increase in lipophilicity. The rate of enzymatic degradation becomes more rapid with increase in chain length. It was also observed that the MRT for GCV was longer with all GCV diesters, which may enable us to lower dosing frequency by twofold resulting in only one injection every 2–3 weeks.

Permeation of xenobiotics across ocular blood vessels into vitreous and aqueous humor is limited due to BOB. It is composed of blood retinal barrier (BRB) and blood aqueous barrier (BAB). These barriers allow selective transport of nutrients in ocular tissues. These transporters can be exploited to improve ocular bioavailability. To delineate the influence of transporters on aqueous and vitreal drug levels, Dias et al. (2003) studied vitreal and aqueous humor elimination pharmacokinetic of ACV, its amino acid prodrug val-acyclovir (VACV) and peptide prodrug val-val-acyclovir (VVACV). ACV, VCAV and VVACV were administered via intravenous infusion in rabbits and aqueous and vitreous humors were sampled by dual probe microdialysis. Aqueous humor showed the presence of ACV 1 h postinfusion and ACV could not reach detectable levels in vitreous chamber. This result clearly indicates that BRB has stronger barrier properties than BAB. VACV and VVACV achieved higher aqueous humor concentrations than parent drug ACV possibly via facilitated transport across BAB. Aqueous humor showed the presence of VACV and ACV but no VVACV was detected. However, VVACV produced highest VACV level in aqueous humor. Both prodrugs could not reach the detectable level in vitreous humor. VVACV had very short plasma half-life due to rapid enzymatic hydrolysis by peptidases to VACV, which may be a possible explanation for the absence of VVACV and the presence of high levels of VACV in aqueous humor. Amino acid and peptide prodrugs of ACV were prepared to target peptide transporters expressed on the BAB. [ $^3\text{H}$ ]Glysar was injected alone and with cold glysar to identify an active transporter system on BOB. Glysar is a known substrate of peptide transporters. Aqueous and vitreous humor levels for glysar were determined and ratios of plasma to aqueous and vitreous humor AUC were calculated (Table 2.2). The penetration ratio (control group) was greater than 1 indicating the presence of peptide transporters on both BRB and BAB. The penetration ratio for aqueous humor decreased significantly when [ $^3\text{H}$ ]glysar was injected with inhibitor (cold glysar). This result confirmed

**Table 2.2** Penetration of [ $^3\text{H}$ ] glycylsarcosine in the presence and absence of inhibitor in rabbits

Rabbits	$\text{AUC}_{\text{aq}}/\text{AUC}_{\text{blood}}$	$\text{AUC}_{\text{aq}}/\text{AUC}_{\text{blood}}$
Control	1.70	1.33
	1.71	1.32
	1.96	2.18
Study (inhibitor)	1.42	1.35
	1.09	2.41
	1.50	1.68
	1.21	1.30

Aqueous penetration ratios of the control group were significantly higher than the study group

the presence of active transport system on BAB. However, penetration ratio for vitreous humor remained unchanged, perhaps due to lower inhibitor concentration due to BRB or higher number of transporters at large surface area of BRB compared to BAB.

BRB also expresses efflux transporters such as P-glycoprotein (P-gp) apart from influx transporter such as PEPT. These transporters can significantly change vitreal clearance if the drug is a substrate of a particular efflux protein expressed on BRB. It has been reported that both BAB and BRB expresses P-gp (Tagami et al. 2009; Duvvuri et al. 2003). Influence of multidrug resistance pumps on ocular drug disposition was investigated using dual probe microdialysis (Duvvuri et al. 2003). Quinidine was employed as a model P-gp substrate, which was administered by both IVT and systemic routes. In vivo inhibition studies were carried out by administering verapamil, which is a known P-gp inhibitor. It was injected intravitreally 20 min before injecting P-gp substrate quinidine. Probes inserted in anterior and posterior segments were also perfused with verapamil in order to ensure P-gp inhibition throughout the study. Verapamil is a calcium channel blocker and may affect the integrity of the BRB. Ocular sodium fluorescein pharmacokinetics was studied after systemic injection alone and in combination with verapamil to show that verapamil does not alter integrity of BRB. In the presence of P-gp inhibitor, the vitreous AUC of quinidine increased twofold after IV administration. It is explicit that P-gp is functionally active on both BRB and BAB on blood side to generate significant effect on pharmacokinetics of quinidine. Vitreal concentration time profile after IVT quinidine, alone and with inhibitor, is shown in Fig. 2.10 and pharmacokinetic parameters are listed in Table 2.3. At high dose, quinidine acts as an inhibitor of P-gp and therefore there was no significant difference in pharmacokinetics when quinidine was administered with or without verapamil. At low dose, quinidine could not reach detectable levels in anterior chamber. In the presence of inhibitor, quinidine AUC decreased by approximately twofold and clearance increased by approximately twofold. In other words, quinidine elimination via transscleral route was accelerated when P-gp was inhibited by verapamil. The pharmacokinetic parameters support the hypothesis that P-gp is present on the inner limiting membrane of retina effluxing the substrates into the vitreous to protect photoreceptors and

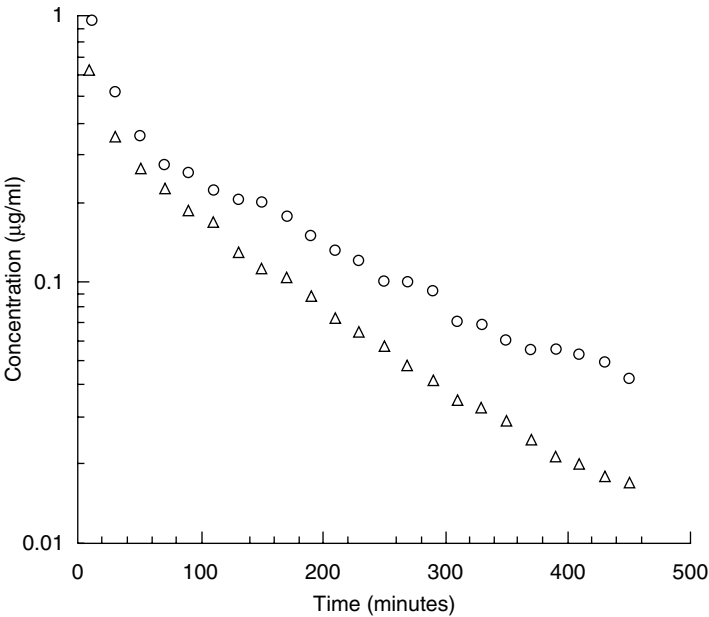


**Fig. 2.10** Vitreal kinetics of quinidine (0.568 µg) following intravitreal administration in the presence (*open triangle*) and absence (*open circle*) of verapamil in the eye

**Table 2.3** Vitreal kinetics of quinidine (0.568 µg) following intravitreal administration in the presence and absence of verapamil in the eye

Parameters	Quinidine	Quinidine + Verapamil
$C_{max}$ (µg/mL)	1.51±0.55	0.66±0.26
$k_{el}$ (min <sup>-1</sup> )	0.0046±0.0005*	0.0072±0.003*
$t_{1/2}$ (min)	152.74±19.31*	96.26±4.7*
$V_d$ (mL)	1.13±0.15	1.30±0.047
AUC (µg min/mL)	110.8±14.17*	61.32±0.17*
CI (mL/min)	0.0052±0.0007*	0.009±0.0001*

\*p<0.05

ganglionic cells on retina. This study provides a clear indication that multidrug resistant pumps work in BOB, keeping xenobiotics out of retina and may significantly alter pharmacokinetics of agents that are substrate of MDR gene products.

Majumdar et al. (2006) studied vitreal pharmacokinetics of peptide prodrugs of GCV after IVT injection using dual probe microdialysis. Vitreal concentration time profile for GCV, Val-GCV, Val-Val-GCV and Gly-Val-GCV were obtained. Prodrugs are inactive molecules which require biotransformation into parent drug to exhibit therapeutic effect. With technique like microdialysis, it was possible to determine the concentration of regenerated active drug as a function of time. Vitreal concentration time profile of Gly-Val-GCV is shown in Fig. 2.11. Figure 2.12 shows comparison between the retinal and vitreal GCV concentrations 8 h post-IVT injection

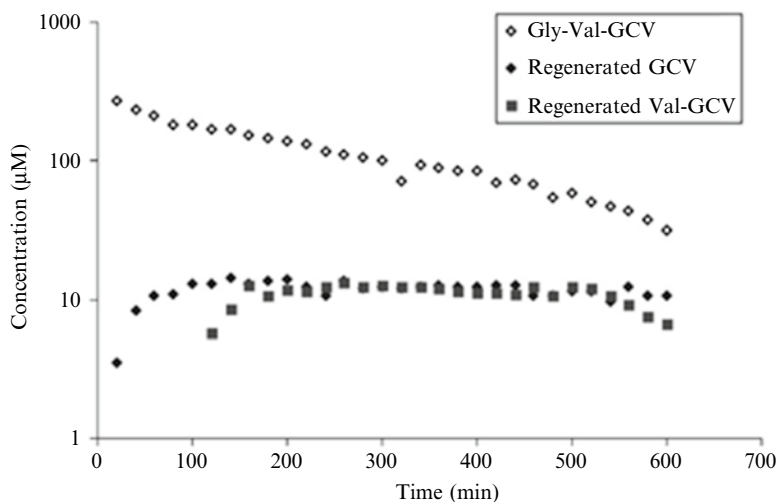


**Fig. 2.11** Vitreous concentration-time profiles of Gly-Val-GCV and regenerated ganciclovir (GCV) and Val-GCV

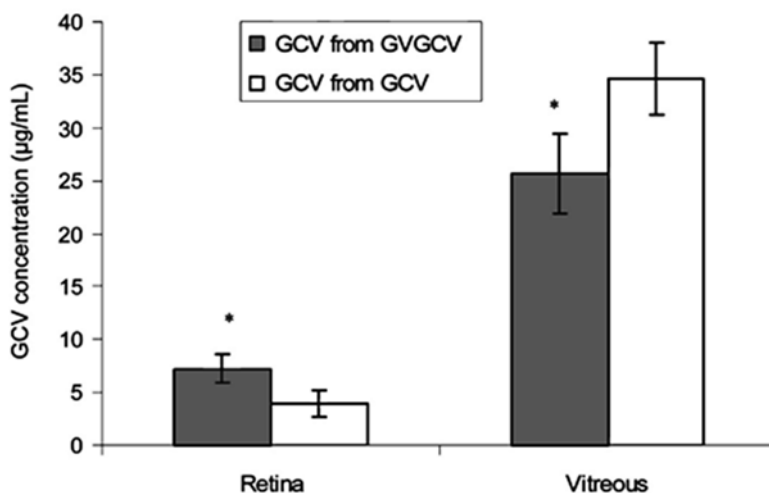


**Fig. 2.12** Retinal and vitreal ganciclovir (GCV) concentrations 8 h postintra-vitreal administration of GCV (control) or Gly-Val-GCV (GVGCV). Values represent mean  $\pm$  standard deviation ( $n=4$ ). \*Represents statistically significant difference from control (Student  $t$  test,  $P<0.05$ )

of Gly-Val-GCV and GCV. The peptide prodrug achieved 1.8-fold GCV level in retina compared to parent drug. Gly-Val-GCV is an excellent prodrug among all the peptide prodrugs, considering vitreal concentration time profile and retinal GCV concentration achieved.



Janoria et al. (2009) developed sodium-dependent multivitamin transporter (SMVT) targeted prodrug of GCV (biotin-GCV) for posterior segment CMV infections. Vitreal pharmacokinetic profile of biotin-GCV was generated to assess involvement of SMVT system in the clearance of prodrug by dual probe anesthetized rabbit model. The aim for developing biotin-GCV was to increase GCV concentration in target retina. Anesthetized animal model has been selected to show evidence of functional activity of transporters in retina. In one such study, Atluri et al. (2008) studied vitreal pharmacokinetics of L-phenylalanine to determine expression and functional activity of large neutral amino acid transporters in rabbit retina.

### 2.4.2 *Conscious Animal Model*

During vitreal microdialysis, the eye is subjected to a mild surgical trauma. The surgical procedure may damage the ocular barriers. *When the BOB is compromised due to surgery and/or inflammation, the obtained pharmacokinetic profile may differ from the one when barrier properties were intact.* Waga et al. hypothesized that if animals are given sufficient recovery period following probe implantation, the effect of surgical trauma, if any, may be reversed. Earlier probes developed for brain microdialysis were made up of stiff metal. Therefore, those probes were not suitable for ocular purposes, especially for chronic usage in conscious animal models. Waga et al. (1991) designed linear probes with soft tubes (outer diameter of 0.6 mm), which can be tolerated by ocular tissue and hence can be utilized for chronic implantation. The dialysis membrane was made up of polycarbonate–polyether copolymer with an inner diameter of 400  $\mu\text{m}$  and MWCO of 20 kDa. With a slightly complicated surgical procedure, microdialysis probe was inserted into vitreous humor, 6 mm below limbus, and dialysis membrane was maneuvered to come close to retina. The tube was fixed onto sclera with sutures. Chloramphenicol ointment (1%) was applied topically to reduce inflammation from surgery. Terramycin® was also added to drinking water for a week after surgery. All the animals were perfused with balanced salt solution to prevent occlusion of probe. The flow rates were 2  $\mu\text{L}/\text{min}$  in pilot series and 4  $\mu\text{L}/\text{min}$  in main series. In vitro and in vivo recoveries were determined to measure the functioning of the probes. Histological analysis was also carried out to examine the anatomical changes in the posterior segment. The probes were well tolerated in most of the animals for few weeks. However, slight inflammatory reactions were seen at the entrance site of probe with retinal folding and detachment in several animals in main series. Several animals developed cataract due to accidental contact of probe with the lens.

In a novel approach to utilize microdialysis technique for chronic drug delivery to posterior segment, Waga and Ehinger (1995) developed conscious animal model in rabbits. Dialysis membrane of polycarbonate and polyamide were studied for net dialysis following probe perfusion with various substrates. The schematic representation of probe positioning in posterior segment is shown in Fig. 2.13. Inlet and outlet of tube were mounted on a stiff plastic tube with dialysis membrane at the

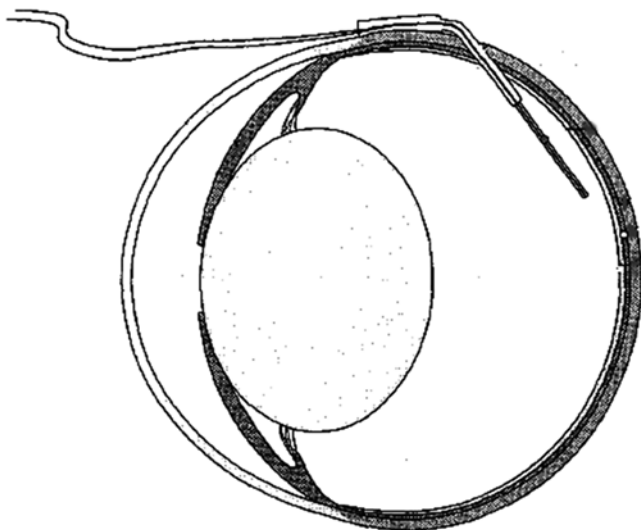


**Fig. 2.13** Schematic representation of probe position in the vitreal chamber of the eye

other end of plastic tube. The concentric design of the probe allows for probe implantation with a single puncture in the globe, decreasing the risk of infection. The probe was inserted via an opening made 4–6 mm below limbus with 0.9 mm cannula and fixed with sutures.

During the procedure, the animals were kept under anesthesia. The probes were perfused at flow rate of 4  $\mu\text{L}/\text{min}$  1 day after surgery. Animals were allowed to recover for a day before any drug administration is initiated (Waga and Ehinger 1995). The probes were well tolerated and remained functional for 20 days on average. Polycarbonate membranes appeared to bind lipophilic drugs at low concentrations, whereas no such affinity was observed with polyamide membranes. Vitreal pharmacokinetics of ceftazidime following intramuscular and IVT routes were studied with this model (Waga et al. 1999). Effects of mild inflammation (mimicking initial stage of endophthalmitis) on vitreal kinetics were also examined. The penetration of ceftazidime was doubled in the eyes with mild inflammation relative to normal eyes. This response may be due to destruction of BRB under mild inflammatory conditions. However, pharmacokinetic parameters obtained after IVT injection were different from intramuscular administration. Variation in the injection site with IVT administration may be responsible for the variation. Also the animals were not anesthetized and therefore their movement may cause slight changes in the angle of the probe.

Usually xylazine and ketamine are used for anesthesia throughout the experiment in anesthetized rabbit models. However, in combination, these compounds have been shown to suppress both heart and respiratory rates. In addition, they can alter IOP. *These side effects related to anesthesia might influence the posterior segment pharmacokinetics.* In anesthetized models, usually 2 h of recovery period

**Table 2.4** Experimental protocol for study of ocular pharmacokinetics and pharmacokinetic parameters of ganciclovir (GCV) after intravitreal administration of [ $^3\text{H}$ ] GCV (50  $\mu\text{L}$ )

		Group I	Group II	Group III
Experimental conditions	Anesthesia	Yes	No	Yes
	Recovery period	No	Yes	Yes
Pharmacokinetic parameters	AUC ( $\mu\text{Ci/mL min}$ )	650.71 $\pm$ 264.70	95.16 $\pm$ 78.58	564.34 $\pm$ 227.67
	Half-life (min)	360.39 $\pm$ 91.16	210.63 $\pm$ 56.77	239.58 $\pm$ 30.72
	AUC ratio compared with Group II	6.84	–	5.93

is allowed. However, this time period may not be sufficient to reverse the changes due to probe implantation. Dias and Mitra (2003) developed a simpler conscious animal model with less tedious surgical procedure using a linear probe to investigate the effects of anesthesia and length of recovery period/probe implantation. Briefly, the eye was proptosed and a linear probe was inserted 8 mm below limbus with a 25-G needle. The probe was slightly angled to avoid contact with lens to avoid cataract formation and was fixed to conjunctiva with suture. The probes were circulated with saline to prevent blocking and also to ensure that probes were not cracked nor had leakage. Animals were divided into three groups as shown in Table 2.4.

A recovery period of 5 days was allowed for groups II and III. Ketamine and xylazine were used for producing anesthesia. Animals in all three groups were given [ $^3\text{H}$ ]GCV (50  $\mu\text{L}$ ) intravitreally. Elevated protein levels in experimental eyes were measured and compared with levels in control eye (contralateral eye) in group I where no recovery period was allowed. Protein level was higher 3–4 times, but levels went down with time. However, increments in protein levels are generally 30–40-fold when BRB is damaged. Also, GCV does not show high protein binding (1–2% protein binding) which means a 3–4-fold increment will not influence pharmacokinetics of GCV. In groups II and III, 5 days were allowed to recover and by this time the protein level reached the baseline. Pharmacokinetic parameters calculated after IVT injection of [ $^3\text{H}$ ]GCV are summarized in Table 2.4. There was a significant increase in AUC in the groups where animals were anesthetized during experiments. Groups I and III animals exhibited sixfold increase in AUC compared to group II. These increments may be attributed to anesthesia which is known to lower heart and respiratory rates. Anesthesia may alter IOP which in turn may change convective forces. Though the vitreal distribution of compounds is diffusion mediated, changes in convective force due to pressure difference in anterior and posterior segment may slow down the distribution of compounds leading to lower amounts of drugs entering retina, thus causing concentration build up in vitreous humor. However, the half-life of GCV in all three groups did not show significant difference indicating that major route of elimination is transretinal in all three groups. Hence, anesthesia primarily alters the distribution of compounds but the elimination rate remains unaffected. For compounds exhibiting high protein binding, the recovery period may be a crucial factor affecting ocular distribution.

*Conscious animal model allows continuous sampling of vitreous humor over several days, usually 20–30 days. Therefore, this technique is very useful for studying*

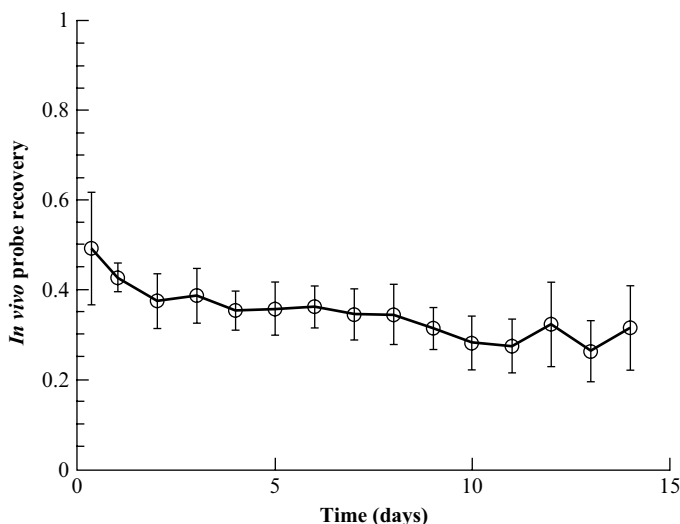


**Fig. 2.14** In vivo probe recovery vs. time profile. Probe recovery is calculated by retrodialysis using acyclovir in perfusate

*pharmacokinetics of sustained release formulation.* Duvvuri et al. (2007) developed GCV loaded poly(DL-lactide-co-glycolide) (PLGA) microspheres for controlled release to the retina. With conscious animal model it was possible to study in vivo drug release from microspheres for 14 days. The model was developed according to the method described in an earlier publication (Anand et al. 2004). Consistency in probe functioning over 14 days was monitored by retrodialysis with ACV as the internal standard (Fig. 2.14).

After a recovery period of 5 days, GCV solution (196  $\mu\text{g}/60 \mu\text{L}$ ) and GCV loaded microspheres (equivalent to 196  $\mu\text{g}/60 \mu\text{L}$ ) were injected intravitreally. The pharmacokinetic parameters obtained for GCV solution were consistent with previously published results. The polymeric microspheres consistently maintained GCV levels at  $\sim 0.79 \pm 0.17 \mu\text{g}/\text{mL}$  which is well above the minimum effective concentration (0.2  $\mu\text{g}/\text{mL}$ ) in vitreous humor for  $\sim 14$  days (Fig. 2.15). The in vitro release profile of the same formulation suspended in poly(DL-lactide-co-glycolide)-poly(ethylene glycol)-poly(DL-lactide-co-glycolide) (PLGA-PEG-PLGA) gel exhibited biphasic behavior for 15 days and triphasic during entire release (Fig. 2.16). On the 15th day approximately 50% of GCV was released. However, in vivo release from microspheres was monophasic during experimental duration ( $\sim 14$  days). The release rate was very slow with only  $33.18 \pm 7.62 \mu\text{g}$  of GCV released over 14 days, which is only  $\sim 17\%$  of total GCV amount. This massive difference in release profile between in vitro and in vivo conditions may be due to significant differences in experimental conditions. For in vitro drug release, the microspheres were suspended in 200  $\mu\text{L}$  of gelling polymer PLGA-PEG-PLGA solution and release was carried out in IPBS buffer at  $37^\circ\text{C}$  and 60 oscillations/min. Thus, release would be faster because of oscillations in buffer with viscosity close to water. For in vivo release following

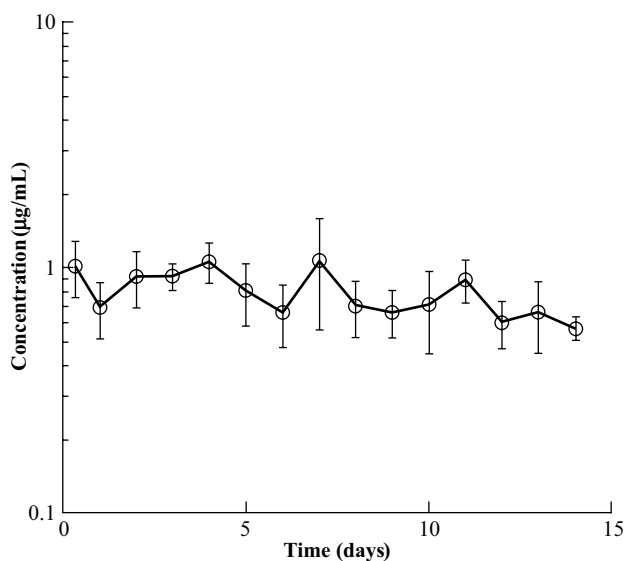


**Fig. 2.15** Vitreal concentration time profile of ganciclovir (GCV) following an intravitreal administration of the mixture formulation (196 µg of GCV)

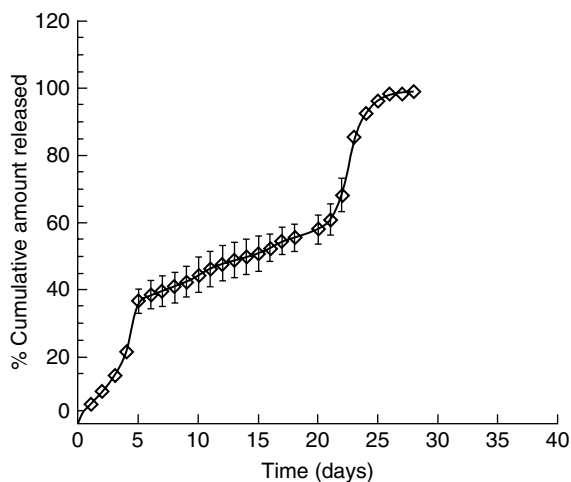


**Fig. 2.16** In vitro release of ganciclovir from 10 mg of 1:1 mixture Resomer RG 502H microspheres and blend microspheres dispersed in 200 µL of 23% w/w aqueous solution of PLGA-PEG-PLGA polymer at 37°C and 60 oscillations/min ( $n=3$ )

IVT injection, microspheres were suspended in vitreous humor, which is a fairly stagnant viscous fluid reservoir. Thus, GCV release would be slower as it is dependent on intrinsic diffusivity of the GCV instead of the amount of dissolved GCV in vitreous. Thus, with permanently implanted probes, it was possible to delineate true release property of microspheres under in vivo conditions.

## 2.5 Vitreal Pharmacokinetics in Animals Other than Rabbits

Rabbits have been the choice of species for vitreal pharmacokinetic studies. However, time to time, various other animal species have also been employed including rats, birds, cats and zebrafish to study physiology of ocular tissues.

Ebihara et al. (1997) measured melatonin levels in pineal and retinal tissues to understand role of melatonin in avian circadian rhythm with permanently implanted microdialysis probes in the eye and pineal gland. After a recovery period of few days, birds were subjected to light–dark cycle and melatonin release was measured. Antiphase relation between dopamine and melatonin release was also confirmed by simultaneous measurements of dopamine and melatonin. In a similar study, Puppala et al. (2004) investigated the effects of light and dark cycles on dopamine release from retina utilizing microdialysis in anesthetized zebrafish. Dopamine release was found to be elevated for transition from dark to flickering light and decreased for shift from flickering light to dark. Shift from dark to steady light and steady light to dark had no influence on dopamine release.

Several investigators have developed microdialysis models with rats despite small size of globe. However, anatomically rat eyes are similar to human eyes and show the presence of highly vascularized retina (Pow 2001). In comparison to rats, rabbits have poorly vascularized retina and most of the dose enters retina via choroidal circulation which is separated from retina by RPE (outer BRB) (Pow 2001; Sen et al. 1992). Katayama et al. (2006) studied the influence of organic anion transporter (OAT) on the passage of estradiol 17- $\beta$ -glucuronide (E17 $\beta$ G) across BRB utilizing microdialysis in an anesthetized rat model. Custom designed concentric probes were inserted in vitreous humor with the help of 25-G needle, 1 mm below limbus. Dialysis tube with MWCO of 50 kDa was employed and probes were circulated with Ringer-HEPES solution at 2  $\mu$ L/min at 37°C. Following probe insertion, [ $^3$ H]E17 $\beta$ G and [ $^{14}$ C]mannitol (marker of paracellular permeability) were injected intravitreally. For inhibition studies, known substrates of OAT were perfused through dialysis probe throughout the experiment and [ $^3$ H]E17 $\beta$ G was given intravitreally. [ $^3$ H]E17 $\beta$ G and [ $^{14}$ C]mannitol showed bi-exponential elimination kinetics from vitreous and [ $^3$ H]E17 $\beta$ G had 1.9-fold higher elimination rate constant compared to [ $^{14}$ C]mannitol. Involvement of OAT system was confirmed with inhibition studies, where elimination rate for [ $^3$ H]E17 $\beta$ G decreased in the presence of OAT substrates such as sulfobromophthalein, probenecid, digoxin and dehydroepiandrosterone sulfate. The elimination rate constant was unchanged for [ $^{14}$ C]mannitol, which indicated a transporter system for [ $^3$ H]E17 $\beta$ G and intactness of BRB. In similar study, Hosoya et al. (2009) employed microdialysis to confirm the functional expression of OAT3 in inner BRB, in rats. In another study, Yoneyama et al. (2010) employed microdialysis and studied vitreal pharmacokinetics of L-proline to identify functional presence of system. A transporter system in retinal blood capillaries is an anesthetized rat model. Thus, rat model offers distinct advantage over rabbit models due to the presence of highly

vascularized retina. This blood supply together with the presence of several transporter systems may considerably influence elimination of various molecules via the transretinal route.

## 2.6 Summary

Microdialysis has become an instrumental sampling technique to study posterior segment pharmacokinetics without sacrificing a huge number of animals. It has undergone significant transformations in the last decade and currently several animal models have been established for sampling inaccessible posterior segment tissues such as vitreous humor. Remarkable progress has been made in the probe design and validation techniques. Ocular microdialysis has been widely utilized in studying drug disposition and determining functional existence of transporters in retina. However, several experimental conditions such as probe design, recovery period, perfusate flow rate, anesthesia, tissue trauma and validation of animal model may influence obtained pharmacokinetic profile. Flow rate should be carefully adjusted to have enough sample volume at particular time points with good recovery in order to avoid issues related to analysis. Anesthesia significantly influences drug elimination by altering IOP, heart rate and respiratory rate. Choice of animal for microdialysis primarily depends on the objective of the study. The tissue damage could result in increased protein concentration or may affect integrity of BRB. The tissue trauma due to probe insertion method may significantly alter the pharmacokinetic profile. The animal model must be validated before performing the studies. The abovementioned parameters should be carefully optimized for studying ocular pharmacokinetics. So far, microdialysis has provided valuable information in the assessment of drug disposition in posterior segment and is expected to provide useful information to develop novel ocular therapeutics.

**Acknowledgment** Supported by National Institutes of Health grants R01EY 09171–16 and R01EY 10659–14.

## References

- Adachi A, Hasegawa M, Ebihara S (1995) Measurement of circadian rhythms of ocular melatonin in the pigeon by in vivo microdialysis. *Neuroreport* 7:286–288
- Adachi A, Nogi T, Ebihara S (1998) Phase-relationship and mutual effects between circadian rhythms of ocular melatonin and dopamine in the pigeon. *Brain Res* 792:361–369
- Amberg G, Lindefors N (1989) Intracerebral microdialysis: II. Mathematical studies of diffusion kinetics. *J Pharmacol Methods* 22:157–183
- Anand BS, Atluri H, Mitra AK (2004) Validation of an ocular microdialysis technique in rabbits with permanently implanted vitreous probes: systemic and intravitreal pharmacokinetics of fluorescein. *Int J Pharm* 281:79–88

- Atluri H, Mitra AK (2003) Disposition of short-chain aliphatic alcohols in rabbit vitreous by ocular microdialysis. *Exp Eye Res* 76:315–320
- Atluri H, Talluri RS, Mitra AK (2008) Functional activity of a large neutral amino acid transporter (lat) in rabbit retina: a study involving the in vivo retinal uptake and vitreal pharmacokinetics of l-phenyl alanine. *Int J Pharm* 347:23–30
- Ben-Nun J, Cooper RL, Cringle SJ, Constable IJ (1988) Ocular dialysis. A new technique for in vivo intraocular pharmacokinetic measurements. *Arch Ophthalmol* 106:254–259
- Dias CS, Mitra AK (2003) Posterior segment ocular pharmacokinetics using microdialysis in a conscious rabbit model. *Invest Ophthalmol Vis Sci* 44:300–305
- Duvvuri S, Gandhi MD, Mitra AK (2003) Effect of p-glycoprotein on the ocular disposition of a model substrate, quinidine. *Curr Eye Res* 27:345–353
- Duvvuri S, Janoria KG, Pal D, Mitra AK (2007) Controlled delivery of ganciclovir to the retina with drug-loaded poly(d, l-lactide-co-glycolide) (plga) microspheres dispersed in plga-peg-plga gel: a novel intravitreal delivery system for the treatment of cytomegalovirus retinitis. *J Ocul Pharmacol Ther* 23:264–274
- Ebihara S, Adachi A, Hasegawa M, Nogi T, Yoshimura T, Hirunagi K (1997) In vivo microdialysis studies of pineal and ocular melatonin rhythms in birds. *Biol Signals* 6:233–240
- Gunnarsson G, Jakobsson AK, Hamberger A, Sjostrand J (1987) Free amino acids in the pre-retinal vitreous space. Effect of high potassium and nipecotic acid. *Exp Eye Res* 44:235–244
- Hosoya K, Makihara A, Tsujikawa Y, Yoneyama D, Mori S, Terasaki T, Akanuma S, Tomi M, Tachikawa M (2009) Roles of inner blood-retinal barrier organic anion transporter 3 in the vitreous/retina-to-blood efflux transport of p-aminohippuric acid, benzylpenicillin, and 6-mercaptopurine. *J Pharmacol Exp Ther* 329:87–93
- Hughes PM, Krishnamoorthy R, Mitra AK (1996) Vitreous disposition of two acycloguanosine antivirals in the albino and pigmented rabbit models: a novel ocular microdialysis technique. *J Ocul Pharmacol Ther* 12:209–224
- Janoria KG, Boddur SH, Wang Z, Paturi DK, Samanta S, Pal D, Mitra AK (2009) Vitreal pharmacokinetics of biotinylated ganciclovir: role of sodium-dependent multivitamin transporter expressed on retina. *J Ocul Pharmacol Ther* 25:39–49
- Kalant H (1958) A microdialysis procedure for extraction and isolation of corticosteroids from peripheral blood plasma. *Biochem J* 69:99–103
- Katayama K, Ohshima Y, Tomi M, Hosoya K (2006) Application of microdialysis to evaluate the efflux transport of estradiol 17-beta glucuronide across the rat blood-retinal barrier. *J Neurosci Methods* 156:249–256
- Louzada-Junior P, Dias JJ, Santos WF, Lachat JJ, Bradford HF, Coutinho-Netto J (1992) Glutamate release in experimental ischaemia of the retina: an approach using microdialysis. *J Neurochem* 59:358–363
- Macha S, Mitra AK (2001) Ocular pharmacokinetics in rabbits using a novel dual probe microdialysis technique. *Exp Eye Res* 72:289–299
- Majumdar S, Kansara V, Mitra AK (2006) Vitreal pharmacokinetics of dipeptide monoester prodrugs of ganciclovir. *J Ocul Pharmacol Ther* 22:231–241
- Maurice DM (1957) The exchange of sodium between the vitreous body and the blood and aqueous humour. *J Physiol* 137:110–125
- Maurice DM (1959) Protein dynamics in the eye studied with labelled proteins. *Am J Ophthalmol* 47:361–368
- Pow DV (2001) Amino acids and their transporters in the retina. *Neurochem Int* 38:463–484
- Puppala D, Maaswinkel H, Mason B, Legan SJ, Li L (2004) An in vivo microdialysis study of light/dark-modulation of vitreal dopamine release in zebrafish. *J Neurocytol* 33:193–201
- Rittenhouse KD, Pollack GM (2000) Microdialysis and drug delivery to the eye. *Adv Drug Deliv Rev* 45:229–241
- Sen HA, Berkowitz BA, Ando N, de Juan E Jr (1992) In vivo imaging of breakdown of the inner and outer blood-retinal barriers. *Invest Ophthalmol Vis Sci* 33:3507–3512
- Stempels N, Tassignon MJ, Sarre S, Nguyen-Legros J (1994) Microdialysis measurement of catecholamines in rabbit vitreous after retinal laser photocoagulation. *Exp Eye Res* 59:433–439



- Tagami M, Kusuvara S, Honda S, Tsukahara Y, Negi A (2009) Expression of ATP-binding cassette transporters at the inner blood-retinal barrier in a neonatal mouse model of oxygen-induced retinopathy. *Brain Res* 1283:186–193
- Ungerstedt U, Pycock C (1974) Functional correlates of dopamine neurotransmission. *Bull Schweiz Akad Med Wiss* 30:44–55
- Waga J, Ehinger B (1995) Passage of drugs through different intraocular microdialysis membranes. *Graefes Arch Clin Exp Ophthalmol* 233:31–37
- Waga J, Ohta A, Ehinger B (1991) Intraocular microdialysis with permanently implanted probes in rabbit. *Acta Ophthalmol (Copenh)* 69:618–624
- Waga J, Nilsson-Ehle I, Ljungberg B, Skarin A, Stahle L, Ehinger B (1999) Microdialysis for pharmacokinetic studies of ceftazidime in rabbit vitreous. *J Ocul Pharmacol Ther* 15:455–463
- Wages SA, Church WH, Justice JB Jr (1986) Sampling considerations for on-line microbore liquid chromatography of brain dialysate. *Anal Chem* 58:1649–1656
- Wang Y, Wong SL, Sawchuk RJ (1993) Microdialysis calibration using retrodialysis and zero-net flux: application to a study of the distribution of zidovudine to rabbit cerebrospinal fluid and thalamus. *Pharm Res* 10:1411–1419
- Yoneyama D, Shinozaki Y, Lu WL, Tomi M, Tachikawa M, Hosoya K (2010) Involvement of system A in the retina-to-blood transport of l-proline across the inner blood-retinal barrier. *Exp Eye Res* 90:507–513

<http://www.springer.com/978-1-4419-9919-1>

Drug Product Development for the Back of the Eye

Kompella, U.B.; Edelhauser, H.F. (Eds.)

2011, XII, 592 p., Hardcover

ISBN: 978-1-4419-9919-1